$GABA_B$ receptor-mediated, layer-specific synaptic plasticity reorganizes gamma-frequency neocortical response to stimulation

Matthew Ainsworth[a,b], Shane Lee[c], Marcus Kaiser[d], Jennifer Simonotto[e], Nancy J. Kopell[f,1], and Miles A. Whittington[a,1]

[a]Hull York Medical School, University of York, Heslington, YO10 5DD, United Kingdom; [b]Institute of Neuroscience, Newcastle University, Newcastle upon Tyne, NE2 4HH, United Kingdom; [c]Department of Neuroscience, Brown University, Providence, RI 02912; [d]Interdisciplinary Computing and Complex Biosystems Research Group, School of Computing Science, Newcastle University, Newcastle upon Tyne, NE1 7RU, United Kingdom; [e]Faculty of Medicine, National Heart and Lung Institute, Imperial College London, London, SW7 2AZ, United Kingdom; and [f]Department of Mathematics and Statistics, Boston University, Boston, MA 02215

Contributed by Nancy Kopell, April 5, 2016 (sent for review November 28, 2015; reviewed by Robert Desimone and Andreas Draguhn)

Repeated presentations of sensory stimuli generate transient gamma-frequency (30–80 Hz) responses in neocortex that show plasticity in a task-dependent manner. Complex relationships between individual neuronal outputs and the mean, local field potential (population activity) accompany these changes, but little is known about the underlying mechanisms responsible. Here we show that transient stimulation of input layer 4 sufficient to generate gamma oscillations induced two different, lamina-specific plastic processes that correlated with lamina-specific changes in responses to further, repeated stimulation: Unit rates and recruitment showed overall enhancement in supragranular layers and suppression in infragranular layers associated with excitatory or inhibitory synaptic potentiation onto principal cells, respectively. Both synaptic processes were critically dependent on activation of $GABA_B$ receptors and, together, appeared to temporally segregate the cortical representation. These data suggest that adaptation to repetitive sensory input dramatically alters the spatiotemporal properties of the neocortical response in a manner that may both refine and minimize cortical output simultaneously.

gamma rhythms | habituation | $GABA_B$ receptor | sensory processing | synaptic plasticity

Gamma-frequency (30–80 Hz) neuronal-population activity is a near-ubiquitous property of cortical responses to all modalities of sensory input (1). It is a feature of the temporal organization of outputs from neuronal ensembles and plays a critical role in intercortical communication and short-term memory (2). However, gamma-frequency responses are not stereotyped; they are powerfully influenced by neuromodulatory state and the nature of the cognitive task associated with sensory presentations. In particular they show plasticity, manifesting as changing local field potential power, frequency, spatial extent, and altered neuronal spike rates and spike-field coherences (3, 4). This plasticity is particularly overt on repeated presentation of familiar or novel discrete sensory stimuli (5–7).

Understanding the processes underlying this plasticity is further complicated by the mechanistic inhomogeneity of brain rhythms within the gamma band. Both the lower (30–50 Hz) and higher (51–80 Hz) subbands are generated by fast spiking interneuronal recruitment into local circuit activity (8). However, in general they originate in different primary sensory cortical laminae and manifest in different cognitive states (9). In addition, although a repetition-related suppression of neuronal response has been most frequently described, notable examples have reported enhancements of both broadband gamma-frequency population activity (10) and discrete neuronal outputs (spikes) (11). Why enhancement or suppression is observed remains unclear. However, the direction of observed plasticity in the sensory gamma-frequency response can be influenced by task (12), stimuli (13), and the pattern of ongoing neuronal activity (5).

Plasticity in the gamma-related cortical representation of a repeatedly presented sensory stimulus has been proposed to underlie cognitive and behavioral improvements during task repetition (14). Enhancement has been suggested to represent greater recruitment of cortex (in terms of neuronal output rates and active area of cortical mantle) involved in encoding of a presented sensory stimulus. In contrast, suppression of neuronal responses may correspond to the "sharpening" (i.e., an increased efficiency) of cortical sensory representation (15, 16). A number of potential mechanisms may account for this sharpening effect, all converging on the pruning of unnecessary information held in the number, and activity patterns, of activated neurons (17). Recent evidence suggests that sharpening and enhancement may reflect different lamina-specific responses to sensory input: layer 4 activation (in response to sensory stimulation) has a predominantly excitatory effect on superficial layer neurons but a predominantly inhibitory effect on deep layer neurons (18).

Despite these observations, little is known about the relevant underlying changes in neuronal communication at the synaptic level—the presumed primary locus for plasticity in the brain (19). This is despite the current understanding of the cellular and synaptic mechanisms required to generate gamma oscillations (20) and their relation to excitatory synaptic plasticity (21). Although extensive literature detailing plastic changes in both excitatory and inhibitory transmission in neocortex (22, 23) complement

Significance

How the brain deals with the barrage of sensory information during wakefulness determines cognitive performance. Strategies include bias toward attending to novel sensory information and an ability to enhance or habituate cortical responses to repeated inputs. Here we show both enhancement and habituation occur simultaneously in different layers of cortex and that the plastic processes involved require activation of the $GABA_B$ subtype of neuronal inhibition. The work demonstrates that the brain can change the way it routes repeatedly presented sensory information in two complementary ways: It optimizes the local cortical representation, including more information as the stimulus is repeated; and it minimizes the output to other areas, preserving only outputs most closely correlated with the local cortical representation.

Author contributions: M.A.W. designed research; M.A. and S.L. performed research; M.A., S.L., M.K., J.S., and M.A.W. analyzed data; and N.J.K. and M.A.W. wrote the paper.

Reviewers: R.D., Massachusetts Institute of Technology; and A.D., University of Heidelberg.

The authors declare no conflict of interest.

Freely available online through the PNAS open access option.

[1]To whom correspondence may be addressed. Email: miles.whittington@hyms.ac.uk or nk@bu.edu.

this understanding, few studies have considered both gamma rhythms and plasticity together (21); thus knowledge of how synaptic plastic changes may subsequently perturb gamma oscillations is limited.

To better understand the role of gamma rhythms in plasticity of cortical sensory representations, we explored lamina-specific changes in local population potentials and discrete neuronal activity in response to repeated layer 4 activation in auditory cortex in vitro. We demonstrate concurrent, highly layer-specific plastic changes in the spatiotemporal properties of gamma rhythms differentially associated with either inhibitory or excitatory synaptic plastic processes: both enhancement of neuronal activity in superficial layers and suppression in deep layers manifested through activation of $GABA_B$ receptors.

Results

Repeat Stimuli Induce Plasticity in Local Field Potential Gamma Rhythm. An initial, transient excitation of the primary auditory cortex granular layer (Au1) induced local field potential (LFP) responses with both a low (30–50 Hz) and high (50–80 Hz) gamma component in all cortical layers of both Au1 and adjacent Au2 (Figs. 1 and 2*A*, *i*). Response durations were 9.3 ± 1.4 s, 11.3 ± 1.4 s, and 9.4 ± 1.2 s in layers 2/3, 4, and 5/6, respectively ($n = 7$). High and low gamma frequency LFP power was maximal in different laminae: High gamma frequency activity was predominant in electrodes located 800 μm from pial surface (corresponding to layer 4). In contrast, low gamma frequency activity was most pronounced in more superficial and deep electrode locations (Fig. 2*B*, *i*).

A second transient excitation, delivered 1 h after the first, induced gamma responses with durations of 10.9 ± 1.1 s, 10.6 ± 1.2 s, and 11 ± 2.8 s in layers 2/3, 4, and 5/6, respectively ($n = 7$). Comparison of the repeated and initial gamma responses to glutamate application revealed a lamina-selective potentiation of low gamma rhythm power (Fig. 2 *A*, *ii*, and *B*, *i*). Normalized low gamma rhythm power was 133.5% [interquartile range (IQR) 120.0–138.4%] and 175.2% (IQR 147.5–211.6%) of the initial response recorded at electrodes in layers 2/3 and 5/6, respectively ($P < 0.05$, $n = 7$ slices, 15 ± 3 and 11 ± 1 electrodes per slice pooled in layers 2/3 and 5/6, respectively). In contrast, no significant change was seen in layer 4: The second stimulus generated gamma rhythms with a normalized power of 112.0% (IQR 79.3–121.7%), compared with the first response ($P > 0.05$, $n = 7$, 6 ± 2 electrodes per slice pooled from this layer).

Control experiments were performed in which artificial cerebrospinal fluid (aCSF) alone (without glutamate) was applied to layer 4. Application of aCSF alone did not induce gamma-frequency enhancement over baseline levels, nor did it induce any changes in rhythmic activity on repeated application. Analysis of 10-s epochs of activity following the first and second applications of aCSF alone revealed no significant variation in normalized low gamma power: layer 2/3 and layer 5/6 powers were 76.0% (IQR 35.4–103.7%) and 102.2% (IQR 56.5–110.5%), respectively ($P > 0.05$, both $n = 4$ slices).

In contrast to the above enhancement of low gamma power on repeated stimulation, no change was evident on examination of high-frequency gamma activity recorded from any cortical layer. The normalized high gamma responses to second stimuli were 111.9% (IQR 64.0–145.5%), 77.6% (IQR 65.5–168.2%), and 123.1% (IQR 75.3–162.5%) of initial stimulus responses recorded from layers 2/3, 4, and 5/6, respectively (all $P > 0.05$, $n = 7$, 10 ± 4, 8 ± 2, and 6 ± 1 electrodes per slice; Fig. 2*B*, *ii*).

Low Gamma-Band Power Changes Were Accompanied by Layer-Specific Modulation of Unit Activity. A total of 382 isolated single units were recorded during the paired responses to glutamate. Pooling all unit recordings by layer did not reveal any significant changes in spiking accompanying the increase in low gamma power in layers 2/3 and 5/6 (Fig. 3*A*). Mean incidence of units activated by cortical stimulation was increased in layers 2/3 and decreased in layers 5/6 (0.39 ± 0.05–0.43 ± 0.05 and 0.27 ± 0.05–0.25 ± 0.05, respectively). However, this trend was not significant ($P > 0.05$, $n = 7$ slices, 52 ± 8 units per slice). Similarly, no significant difference in median spike rates was seen in each of the layers ($P > 0.05$, $n = 7$ slices, 48 ± 8 units per slice).

Underlying the lack of significant changes in unit behavior overall was a highly lamina-specific, mixed pattern of suppression and enhancement of single unit responses as seen before in vivo (11) (Fig. 3*B*). A total of 177 units showed an enhanced firing rate on presentation of the second stimulus or appeared de novo only on second stimulus presentation: The fraction of these enhanced units in a given layer compared with enhanced units in all layers was 0.53 ± 0.06 for layers 2/3. This was significantly greater compared with layer 4 (0.22 ± 0.04) and layers 5/6 (0.25 ± 0.07, Fig. 3*C*, $P < 0.05$, $n = 7$). In contrast, units that showed reduced spike rates, or were silent, on second stimulus presentation ($n = 122$ suppressed units) were recorded predominantly from

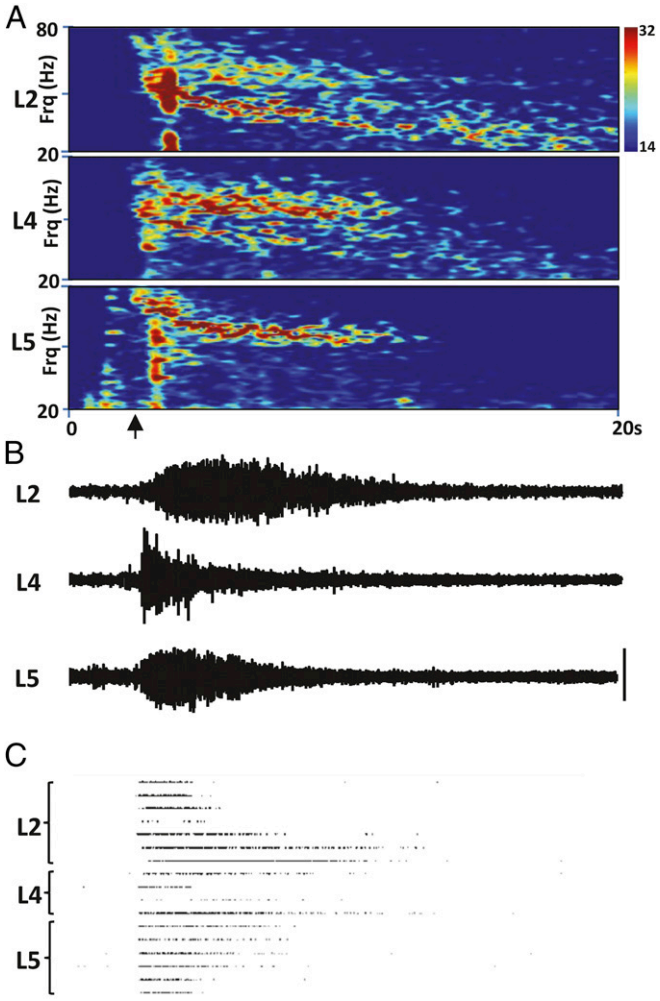

Fig. 1. Individual example of the response to glutamate application. (*A*) Spectrograms of the response to a single (initial) glutamate application to layer 4 at the time indicated by the arrow on the *x* axis. Note both the lamina-selective appearance of the high and low gamma bands as seen previously (33) and the gradual reduction on center frequency of each band as the response progresses. (*B*) Example LFP data from each layer demonstrating the different temporal pattern of magnitude changes as the response progresses (layer 4 initially highest, layers 2/3 and 5 building more slowly. (*C*) Example showing a selection of units from each layer that responded strongest to the glutamate application. (Scale bar in *B*, 50 μV.) LFP traces and unit rasters are aligned to the time axis in *A*.

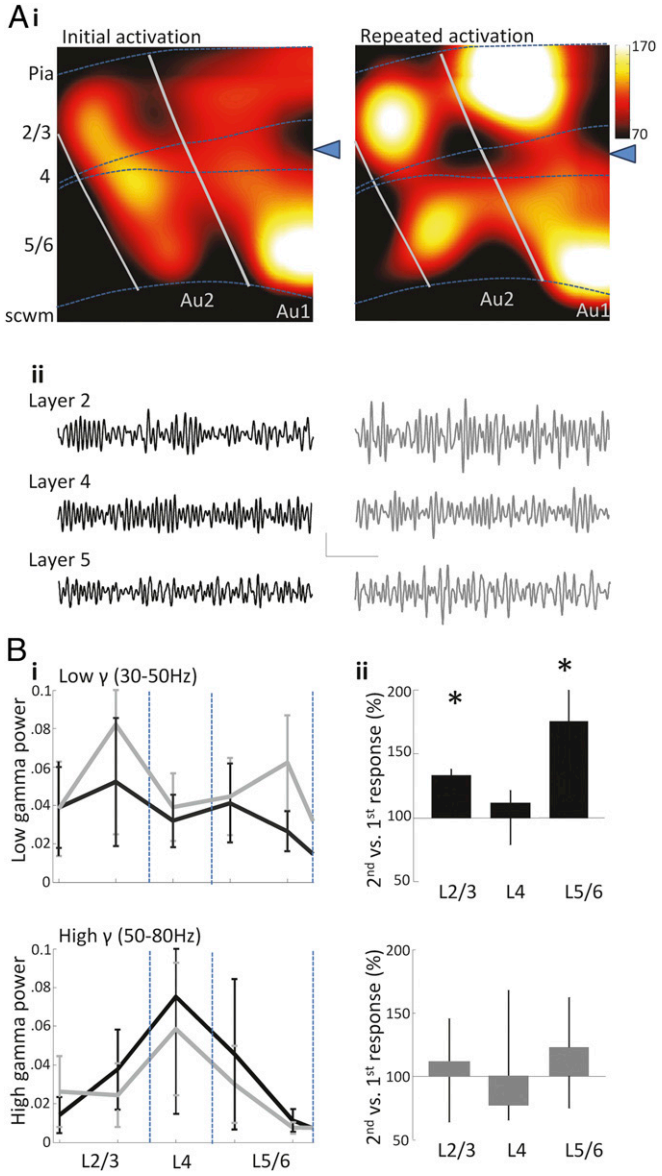

Fig. 2. Repeated application of glutamate to Au1 layer 4 selectively potentiates low gamma frequency activity. (*A*, *i*) Color maps showing the gamma band (30–80 Hz) activity in the primary and secondary auditory cortex induced following the application of glutamate (delivery site denoted by the blue triangle). Dotted lines represent the approximate boundaries of layer 4. (*ii*) Example traces of gamma responses to the initial (*Left*) and the repeated (*Right*) application of glutamate recorded at electrodes in layers 2/3, 4, and 5/6. Calibration, 30 μV, 200 ms. (*B*, *i*) Laminar profiles showing the mean power of low gamma (30–50 Hz) and high gamma (50–80 Hz) activity in response to the initial (black) and repeated (gray) application of glutamate. Laminar profiles show a potentiation of low gamma activity in the second response to glutamate not seen in high gamma activity. (*ii*) Summary of the second response to glutamate normalized to first response to glutamate for low (*Upper* plot) and high (*Lower* plot) gamma (*$P < 0.05$ vs. initial response).

layers 5/6 (0.51 ± 0.09 of all units). The fraction of suppressed units was significantly lower in layer 4 and layers 2/3 (0.18 ± 0.05 and 0.26 ± 0.05 respectively, $P < 0.05$ compared with layers 5/6, $n = 7$ slices; Fig. 3*C*, *i*).

This superficial/deep layer difference in fraction of enhanced or suppressed units on second stimulus presentation was also apparent when considering the magnitude of spike rate changes (Fig. 3*C*, *ii*). Examination of enhanced units revealed the highest increase in firing rates for units in layers 2/3 on second compared with first stimulus presentation [592.7% (209.7–1970.9%)]. This was significantly higher than the rate increase seen in enhanced units in layers 5/6 [234.1% (161.6–501.5%), $P < 0.05$, $n = 68$ and $n = 42$ units, respectively]. Conversely, a significantly more pronounced spike rate reduction was seen in suppressed units in layers 5/6 [second compared with first response 3.6% (0.0–28.2%)] compared with layers 2/3 [25.7% (6.6–58.4%), $P < 0.05$, $n = 34$ and $n = 68$, respectively]. No changes were seen relative to layer 4.

To investigate any relationship between the changes in gamma frequency LFP power and the above reorganization of active units and their spike rates, we examined spike-triggered LFP average waveforms for enhanced and suppressed units within layers 2/3 and 5/6 (Fig. 4 *A* and *B*). In layers 2/3, spike-triggered waveform averages for all pooled spikes had spectra that clearly

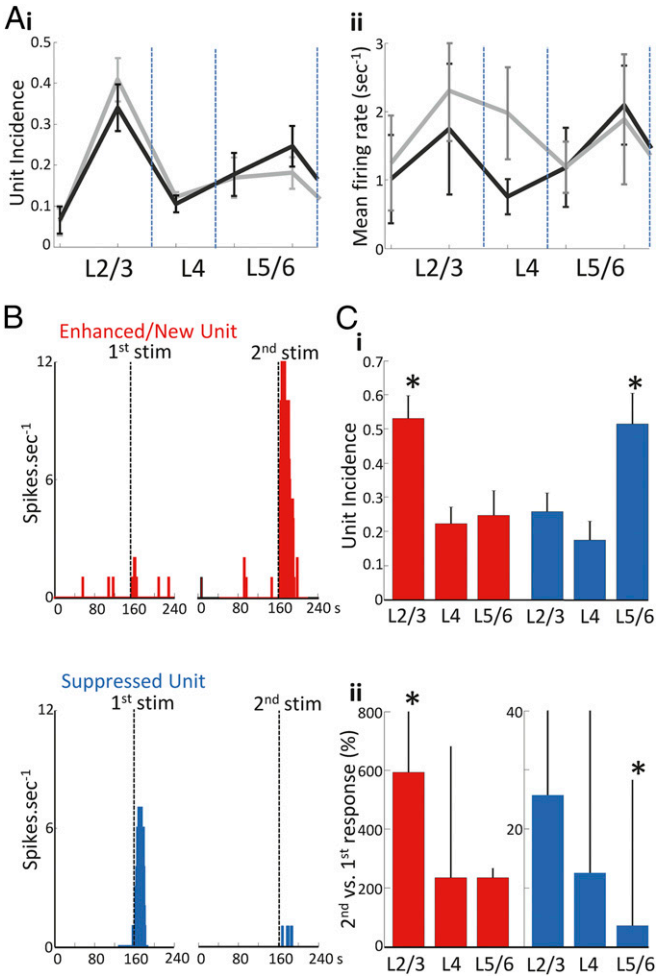

Fig. 3. Glutamate application induces lamina-specific potentiation and suppression of putative pyramidal cell firing. (*A*) Laminar profiles showing (*i*) the incidence of all units across the neocortex and (*ii*) the mean firing rate during both the initial (black) and the repeated response (gray) to glutamate. Pooled analysis of all isolated single units did not reveal significant changes between the initial and repeated glutamate response. (*B*) Example frequency plots of single units demonstrating enhanced (red) and suppressed (blue) activity relative to the initial response. (*C*, *i*) The median lamina-specific fraction of enhanced and suppressed units revealed enhanced units predominant in layers 2/3 with suppressed units in layers 5/6 (*$P < 0.05$). (*ii*) Median unit firing rates during the second response to glutamate vs. the first response to glutamate showed the degree of enhancement to be strongest in superficial vs. deep layers and suppression strongest in deep vs. superficial layers (*$P < 0.05$).

showed two components of the gamma rhythm, with modal peaks at approximately 30 Hz and 50 Hz for the first stimulus presentation only (Fig. 4*A*, *i*). Separation of relative spike/LFP coherences for subsequently enhanced and suppressed units revealed a significantly greater degree of spike/LFP coherence for enhanced units in the middle of the low gamma band (35–45

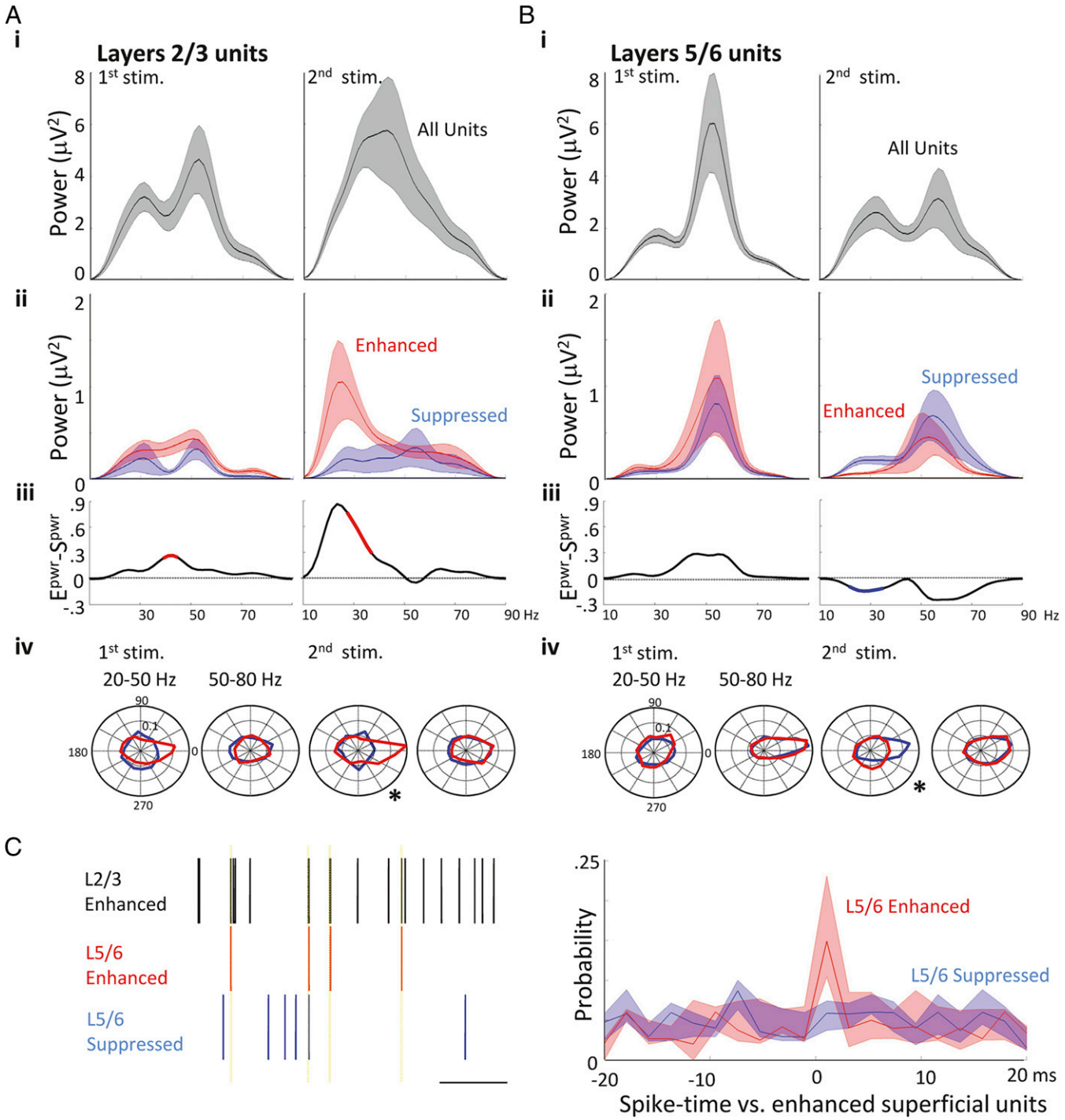

Fig. 4. Enhancement and suppression of unit activity was associated predominantly with units phase locked to low frequency gamma rhythms. (*A*) Spectra calculated from spike-triggered LFP averages (STA) of all units (*A*, *i*, black), enhanced (red), and suppressed (blue). (*A*, *ii*) Superficial units. Differences in the frequency content of the spike-triggered LFP derived from enhanced and suppressed spikes (E^{pwr}–S^{pwr}) are shown in *A*, *iii* with significance determined by Monte Carlo testing against randomized surrogate data (*Methods*). Significant portions of the difference spectra are shown in red (enhanced > suppressed) or blue (suppressed > enhanced, $P < 0.05$). (*A*, *iv*) Polar plots of mean spike phase distribution relative to band-pass filtered low (20–50 Hz) and high (50–80 Hz) gamma responses. Data from enhanced units (red) and suppressed units (blue) revealed significant differences between phase locking only to the low gamma field (*$P < 0.05$). (*B*) Spectra calculated from STAs of all units (black), enhanced (red), and suppressed (blue) deep layer units. Data in *B*, *i–iv* were derived as in *A*, but using units identified in layers 5/6. (*C*) Illustration of spike rasters for three concurrently recorded units during response to glutamate stimulation. Note the greater incidence of synchronous generation of spikes in layers 5/6 enhanced vs. suppressed units, compared with layers 2/3 enhanced units, is shown. (*Right*) shows pooled median probability scores for this measure of enhanced superficial spike – deep spike coherence.

Hz, $P < 0.05$, $n = 23$ enhanced units and $n = 24$ suppressed units; Fig. 4*A*, *iii* and *iv*).

Tracking the fate of these enhanced units during the second response revealed a near-abolition of spike/LFP coherence at the higher end of the gamma band, but a very strong relationship between spike timing and the LFP at lower frequencies. This coupling was significantly higher than during the initial response at 27–37 Hz and integrated power within this frequency band increased fourfold [0.0647 (0.0175–0.394) vs. 0.256 (0.0698–0.736) $\mu V^2 \cdot Hz^{-1}$, $P < 0.05$, $n = 23$ units first response and $n = 41$ units second response, respectively, Fig. 4*A*, *iii* and *iv*]. This peak was absent from spectra of suppressed units during the second response to glutamate ($P < 0.05$, $n = 25$ suppressed units and $n = 41$ enhanced units); additionally suppressed unit LFP coherences showed no significant changes across the entire gamma band between first and second stimulus presentation ($P > 0.05$, $n = 24$ units first response and $n = 25$ units second response).

In layers 5/6, both enhanced and suppressed units demonstrated strong spike/LFP coupling at high gamma frequencies during the initial response, with no significant difference evident between spike/LFP spectra ($P > 0.05$, $n = 23$ suppressed units and $n = 22$ enhanced units; Fig. 4*B*, *ii*–*iv*). In contrast to layers 2/3, enhanced units in layers 5/6 showed no change in spike/LFP relationship across the gamma band during the initial and repeated response ($P > 0.05$, $n = 22$ units first response and $n = 25$ units second response). Suppressed units in layers 5/6 again exhibited spike/LFP coupling at high (>50 Hz) gamma frequencies during the second response. However, a statistically significant increase in the spike-field coupling at low gamma frequencies (between 25–33 Hz) was seen for suppressed units during response to second glutamate presentation ($P < 0.05$ $n = 21$ first response and $n = 20$-s response; Fig. 4*B*, *iii* and *iv*).

Previous work has suggested layer 5/6 gamma rhythms are not generated locally (24) (*Discussion*). Instead these deep layers respond to the frequencies of output from more superficial layers (high gamma from layer 4, low gamma from layers 2/3). To try to understand the mechanism for spike enhancement and suppression in layers 5/6, we compared spike timing in this layer with that of enhanced units in layers 2/3 ($n = 7$ slices, 12 ± 3 units per slice). During the initial response to glutamate, enhanced units in layers 5/6 spiked with highest probability within a short (within the 2-ms bin width) time delay of enhanced unit firing in layers 2/3 (Fig. 4*C*). This interlaminar spike timing relationship was absent from the firing of suppressed units in layers 5/6. Peak probability of enhanced layer 5/6 units spiking within 1 ms of enhanced layers 2/3 units was 0.15 (IQR 0.10–0.24) and for suppressed layers 5/6 units 0.058 (0.04–0.074) ($P < 0.05$, $n = 7$ slices).

To further characterize the laminar redistribution of unit recruitment, we examined spike-triggered averages of the LFP waveforms for layers 2/3 and 5/6 enhanced and suppressed units. These were then correlated with each other and to those for input layer 4 units (Fig. 5*A*). Phase relationships between pairwise spike-triggered correlations were remarkably uniform during response to first stimulus presentation (Fig. 4*B*, black dots), with all LFP components within and across all layers being within approximately 5 ms of each other.

However, on second stimulus presentation, this close temporal relationship only survived for three of the data pairs: These consisted of the LFPs averaged to enhanced units in layers 2/3 and 5/6 and units in layer 4. In contrast, phase relationships for other data pairs were temporally shifted to such an extent that synchrony estimates (the magnitude of the cross-correlogram at 0-ms lag) were not significantly different from equivalent phase-shuffled pairs ($P > 0.05$) or, in the case of suppressed units in layers 2/3 and 5 and layer 4, significantly negative (Fig. 5*B*). Plotting these synchrony estimates in cartoon form (Fig. 5*C*) showed a pattern of change wherein the local field (population) potentials associated with enhanced units became, in general,

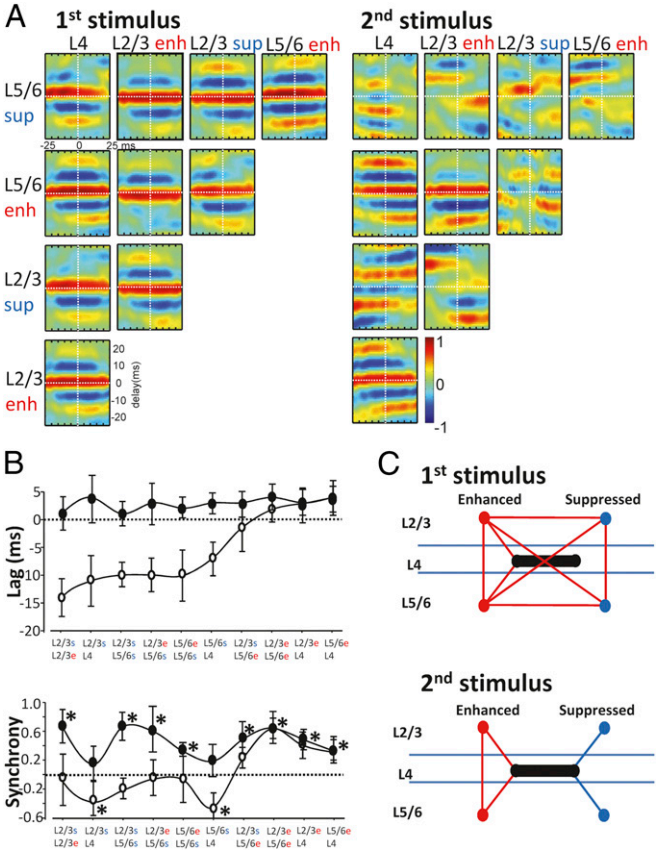

Fig. 5. Spike-averaged LFP waveforms reveal temporal separation of enhanced and suppressed unit-related population activity. (*A*) Matrix of pairwise cross-correlograms of spike-averaged field potentials (STA) during the responses to first (*Left*) and second (*Right*) stimuli. Only delays of −25 ms to +25 ms are shown, plotted for 50 ms centered on the mean spike time. Color map represents the magnitude of the correlation for a given delay at a given time relative to the spikes used for averaging the field potentials. Data plotted is the spike-averaged field cross-correlation for each unit type (deep, superficial, enhanced, and suppressed) ($n = 17$–25 units per slice; $n = 5$ slices). Note all layer 4 units were pooled per slice as no significant enhancement or suppression pattern was seen in this layer. (*B*, *Upper* graph) Mean (± SE mean) values of phase lag/lead for each pair are indicated. Data from responses to first stimulus are filled circles. (*Lower* graph) Mean (± SE mean) synchrony estimates derived from the magnitude of the cross correlation at 0 ms (* denotes significantly different from correlation values for phase shuffled data pairs). (*C*) Cartoon summarizing the synchrony estimates in *B*. Positive synchrony values are represented as red lines between data pairs; negative or zero mean values are shown as blue lines.

temporally separated from those associated with suppressed units. Furthermore, the LFPs associated with suppressed units in layers 2/3 and 5/6 also became temporally separated from each other and from layer 4.

Layer-Specific Inhibitory and Excitatory Long-Term Potentiation Accompanies Plastic Changes in Gamma Power and Unit Responses. The contrasting dominance of spike enhancement in layers 2/3 and suppression in layers 5/6 suggested different underlying plastic processes at the local network level, with mismatched plastic changes possibly contributing to the temporal separation of enhanced and suppressed units seen above. We therefore examined the relative plastic changes in two major local circuit pathways: excitatory synaptic inputs to excitatory cells and inhibitory synaptic inputs to excitatory cells. Electrically stimulated excitatory postsynaptic potentials (EPSPs) recorded from principal cells in layers 2/3 were significantly potentiated 1 h after the

initial glutamate stimulation (pre 4.7 ± 0.3 mV vs. post 7.5 ± 1.1 mV, $P < 0.05$, $n = 5$; Fig. 6*A*). This potentiation was layer specific, not being evident in EPSPs recorded from principal cells in layers 5/6 where unit suppression dominated (pre 4.0 ± 0.3 mV vs. post 4.3 ± 0.4 mV, $P > 0.05$, $n = 5$). In contrast, inhibitory postsynaptic potentials (IPSPs) electrically induced in pyramidal cells in layers 5/6 were strongly potentiated (pre −3.1 ± 0.5 mV vs. post −12.7 ± 3.2 mV, $P < 0.05$, $n = 6$; Fig. 6*A*). Again, this was a layer-specific effect. This plastic change was not seen for IPSPs in layers 2/3 (pre −3.3 ± 0.6 mV vs. post −4.1 ± 0.2 mV, $P > 0.05$, $n = 5$). No significant changes in either EPSPs or IPSPs was seen for layer-4 principal cells ($P > 0.05$).

Synaptic Plastic Changes, Gamma Power, and Unit Plasticity Were Mediated by Activity of $GABA_B$ Receptors. Whereas long-term potentiation of IPSPs and EPSPs can involve the activation of a number of receptors, studies have suggested that $GABA_B$ receptor activation may be an important mediator of both (25, 26). Bath application of the postsynaptic $GABA_B$ receptor antagonist CGP 35348 [(3-Aminopropyl)(diethoxymethyl)phosphinic acid, 50 μM] significantly attenuated both the layers 2/3-specific potentiation of EPSPs (5.6 ± 0.5 mV pre- and 6.0 ± 0.6 mV postglutamate, $P > 0.05$, $n = 5$; Fig. 6*B*) and layers 5/6-specific potentiation of IPSPs (−4.8 ± 0.7 mV pre- and 7.4 ± 1.4 mV postglutamate, $P > 0.05$, $n = 5$; Fig. 5*A*).

To estimate the potential role of the $GABA_B$-dependent synaptic plasticity seen, we examined the effects of CGP 35348 on the main plastic changes seen in field oscillations and units. The presence of CGP 35348 did not significantly alter the durations of gamma responses for the first glutamate stimulus [9.3 ± 1.4 s vs. 10.0 ± 2.1 s, 11.3 ± 1.4 vs. 12.2 ± 1.9 s, for layers 2/3, 4, and 5, respectively ($P > 0.05$, $n = 7$, $n = 5$)]. No significant effect on gamma power in either subband in each layer was seen with CGP 35348 either [28.2 ± 3.8 μV^2 vs. 32.4 ± 4.9 μV^2, 18.1 ± 2.2 μV^2 vs. 15.6 ± 3.2 μV^2, 12.1 ± 2.8 μV^2 vs. 14.7 ± 3.9 μV^2 for layers 2/3, 4, and 5 low gamma power, respectively ($P > 0.05$)]. Layers 2/3 and layer 4 field gamma power changes with the second glutamate stimulus also did not significantly change from control values [128.8% (96.0–148.2), 94.5% (82.3–104.5), respectively, $P > 0.05$, for control values see above; Fig. 6*B*, *i*]. However, the large increase in layers 5/6 low gamma power on second stimulation was significantly reduced on $GABA_B$ receptor blockade. The control increase of 175.2% (147.5–211.6) was changed to 111.4% (80.1–131.3) ($P < 0.05$, $n = 5$; Fig. 6*B*, *i*). Unit plasticity scores (a combination of the increase or decrease in unit numbers and their change in firing rate during the response to glutamate) were also reduced by the $GABA_B$ receptor antagonist. Despite seeing no significant change in the field gamma power increase in layers 2/3, CGP 35348 did significantly reduce layers 2/3 median unit plasticity score from 3.7 (2.0–5.8) to 0.8 (0.1–1.2) for enhanced units ($P < 0.05$; Fig. 6*B*, *ii*). Accompanying the abolition of layers 5/6 gamma power increase, $GABA_B$ receptor blockade also abolished the powerful unit suppression seen in these layers. Control plasticity score for suppressed units was −9.8 (−11.9 to −6.2). This was reduced to −0.7 (−2.3 to −0.2) in the presence of CGP 35348 ($P < 0.05$).

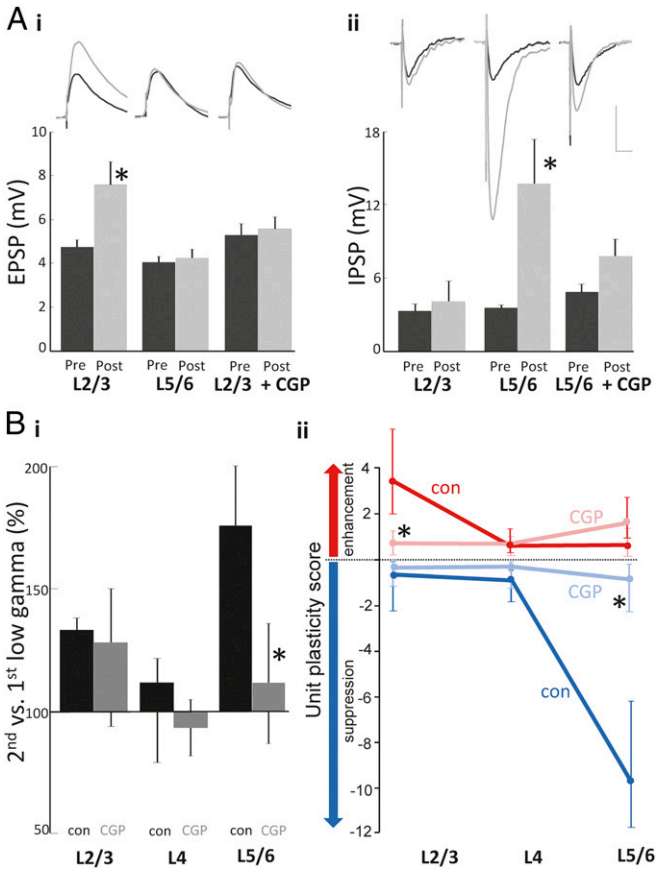

Fig. 6. $GABA_B$ receptors mediate lamina-specific, gamma rhythm-associated plasticity. (*A*) Effects of glutamate stimulation on basic synaptic transmission. (*i*) Average waveforms of electrically stimulated EPSPs recorded from pyramidal cells located in layers 2 and 3 and layer 5 (average from 20 events). Cells held at −80 mV to record EPSPs from cells pre- (black) and 1 h post (gray)-glutamate application. (*Lower*) Summary graph of plastic changes in mean (±SE mean) EPSP amplitude before and 1 h after glutamate application, $P < 0.05$, $n = 5$. Control responses were compared with those in the presence of the $GABA_B$ receptor antagonist CGP 35348 (50 μM, CGP). (*ii*) Average waveform of electrically stimulated PSPs recorded from pyramidal cells located in layers 2 and 3 and layer 5 (averaged from 20 events). Cells were held at −30 mV in the presence of NBXQ (40 μM) and CPP (50 μM) to record IPSPs pre- (black) and 1 h post (gray)-glutamate application. (*Lower*) Summary graph of plastic changes in mean (± SE mean) IPSP amplitude following glutamate application, $*P < 0.05$, $n = 5$. (Scale bar, 3 mV and 20 ms.) (*B*, *i*) The effects of CGP 35348 on the percentage change in median, layer-specific low-frequency gamma field potential power. Note the absence of an effect on the superficial layer potentiation but a near abolition of the deep layer gamma potentiation. (*B*, *ii*) Unit plasticity scores (a combination of unit incidence and firing rate changes; see *Methods*) in the presence (light colors) and absence (dark colors) of CGP 35348 for enhanced units (red) and suppressed units (blue) in the three layer groups. Note $GABA_B$ receptor blockade significantly ($*P < 0.05$) ablates both the superficial enhancement of unit activity and the deep layer suppression.

Discussion

This simple in vitro model of repeated ascending cortical activation captured three key elements of the plasticity in cortical representations of sensory inputs seen in vivo: First, gamma rhythm power was increased—specifically in the low gamma range—with no significant changes to high gamma power. Second, both enhanced and suppressed spike rates were seen, with a clear laminar separation such that superficial layer units were more likely to be enhanced and deep layer units suppressed on repeated stimulation. Third, the enhanced unit spikes were more likely to be phase locked to low frequency gamma rhythms than suppressed spikes (at least in superficial layers). In addition, the model showed that this response plasticity served to temporally separate enhanced from suppressed units. Thus, in terms of cortical assemblies as a substrate for sensory coding, the response was sharpened via two synergistic phenomena: First, a subset of units reduced their likelihood of participating in an assembly through reduced spike rates; and second, remaining spikes from these suppressed units failed to temporally correlate with the main (enhanced) unit population.

Relating these main findings to (mainly visual) in vivo and human data suggests a correlation between some, but not all, previous data. The enhanced gamma power seen here has been reported

in a number of studies (5, 10, 27) but not in all (3–7), with the likelihood of seeing enhancement very tightly related to the nature of the stimulus, repetition frequency, and the nature of any distractors included (5). In the present study, the interstimulus interval was much longer than those used in vivo. This was done deliberately to allow only long-term plastic changes to be manifested. Thus, any short-term remodeling of functional local cortical circuits, such as those underlying the "fatigue" hypothesis (28) cannot be considered to play a role here.

The overall absence of a change in putative principal cell spiking seen in the present study was consistent with the findings of Brunet et al. (5). These authors also reported a selective modification of spike–gamma field synchrony depending on the strength of stimulus drive received, which was similar to the spike/field phase coupling and interlaminar spike–spike coupling seen in the present in vitro experiments (Fig. 4). These data therefore lend further support to the idea of plastic changes due to repetitive stimuli enhancing the efficiency of subsequent cortical representations by increasing synchrony of neurons carrying the most salient information (17). This enhancement process may be, at least in part, a consequence of enhanced top-down inputs to sensory areas at lower frequencies (27, 29, 30). However, as no higher-order, associational areas were present in the slices used here, it can be assumed that such influences are not necessary to manifest the basic plastic changes most commonly reported on repeated sensory stimulation.

These data raise two main questions: What mechanism(s) may underlie the seemingly opposing, lamina-specific changes seen, and what advantage, if any, does this pattern of plasticity confer on neocortex when coding for repeated sensory inputs?

In auditory cortex, the local neuronal circuits in superficial layers are necessary and sufficient for generation of lower frequency gamma rhythms in auditory cortex (31), and the frequency of the local population rhythm is proportional to the output from excitatory neurons (32). Interaction between this slow gamma superficial layer rhythm and the more dominant fast gamma in layer 4 may provide sufficient, appropriate pre- and postsynaptic activity timing to generate excitatory synaptic potentiation onto excitatory neurons (21, 33). However, to optimize excitatory synaptic potentiation, fast, $GABA_A$ receptor-mediated inhibition must not be too high (34). Postsynaptic inhibitory strength is, in part, self-limiting through the action of release GABA on presynaptic $GABA_B$ autoreceptors (25, 35). In superficial neocortical layers, this disinhibition may be compounded on receipt of sensory input by the activity of VIP-immunopositive interneurons that selectively target fast spiking interneurons (36). Disinhibitory interneurons may also use activation of $GABA_B$ receptors to generate their effects (37).

The present data demonstrated that enhanced spiking in superficial layers was associated with a superficial layer-specific long-term (1 h) potentiation of excitatory synapses onto excitatory neurons. This observation was consistent with the predominantly excitatory nature of layer 4 influence on superficial layer neurons (18). Both the spike enhancement and the excitatory synaptic plasticity were almost abolished in the presence of a $GABA_B$ receptor antagonist (Fig. 6).

Synchronous spike generation in superficial layers has been shown to be critical for combining different streams of sensory information. Layer 2/3 neurons are strongly connected to layer 5 neurons (38) so we need also to consider any changes in deeper layers with respect to the above layer 2/3 changes. Layer 5 local circuits (at least in auditory cortex) do not appear to support gamma rhythm generation alone (24) and, in contrast to the superficial layers, receive a predominantly inhibitory input from layer 4 (18). No change in layer 5 EPSP strength was seen in the present study. Whether or not excitatory plasticity occurs at this locus appears to depend on the degree of backpropagation of action potentials in these neurons (39). This backpropagation, in turn, is very much dependent on the level of synaptic inhibition the cells receive (40). This suggests that the dramatic increase in synaptic inhibition in only layer 5 principal neurons seen here may serve to actively prevent recurrent excitatory plasticity in response to repeated stimulation (Fig. 6).

As shown in the present study, inhibitory synaptic inputs to layer 5 principal cells are highly plastic (41). This plasticity is affected by sensory input and has been shown to be involved in long-term local circuit behavior during development (42), habituation to repetitive stimuli (43), and selective optogenetic stimulation of layer 4 neurons (18). However, this latter study implicated layer 4 cell-mediated fast synaptic excitation of layer 5 interneurons in the dominance of inhibition in this layer during sensory input. In the present study, we pharmacologically removed fast synaptic excitation but still saw large increases in synaptic inhibition in this layer. This implicated a locus of plasticity directly at the inhibitory synapse onto layer 5 principal cells. Such plastic potentiation of fast synaptic inhibition is critically dependent on $GABA_B$ receptor activation (44). It has been shown that the patterns of postsynaptic excitatory activity in layer 5 pyramidal cells needed to generate inhibitory input plasticity—short bursts of action potentials—need not also modify excitatory input (i.e., inhibitory synaptic potentiation onto pyramidal cells can occur without concomitant excitatory plasticity as seen in the present experiments) (45). Such a pattern of burst outputs is common in this neuron subtype during gamma rhythms in auditory cortex (24). Interestingly, this form of inhibitory synaptic plasticity did not require precise timing of pre- and postsynaptic excitatory neuronal spiking (46), but potently narrowed the integration window for input summation and enhanced output temporal precision once established (45, 46).

The data presented here therefore indicate that two different forms of synaptic plasticity (both expressed in a $GABA_B$ receptor-dependent manner) occur on cortical activation. Their locus in different laminae, their differential association with spike outputs, and their relationship to low-frequency gamma rhythms on repeated cortical activation, all suggest a profound change in the local cortical representation to repeat stimuli. The changes seen may subserve multiple, computationally useful roles, but two, in particular, seem relevant for habituation to repeated sensory stimuli (47). First, enhanced unit activity and gamma power in superficial layers have been shown to be a vital component of sensory adaptation (3–7, 48). The present data therefore suggest that, for an initial stimulus presentation, long-term potentiation of excitatory synaptic inputs onto superficial layer pyramidal cells enhanced their response to repeated presentation in a manner consistent with the "formation" stage in the Martens and Gruber (47) model. In other words, the more a sensory input is repeatedly presented, the stronger (and thus perhaps more detailed) the neuronal representation of the stimulus in supragranular layers (10–16).

Second, despite this increase in superficial layer neuronal involvement, the enhanced inhibition (and associated gamma rhythm) in the main output layer 5 suggests a sharpening process: the narrowing of the neuronal integration window (above) and overall reduced spike rates, a process similar to that reported for repetitive visual stimulus presentation in the inferior temporal cortex (6, 15). Taken together the present data suggest that the local cortical representation of a repeated stimulus can grow concurrently with a decrease in the output from the region "holding" that local representation; the remaining output is from neurons whose spikes most closely temporally match the representation held in superficial layers. Such "real-time" interactions between selective suppression, enhancement, and increased temporal precision (sharpening) of neuronal outputs has been suggested to be vital for appropriate short-term memory formation and subsequent attentional changes (15).

How the auditory cortex actually "decides" which neuronal activity pattern to keep is a difficult question to answer. The greater association of enhanced units in layers 2/3 with low-frequency gamma rhythms suggests the precise spike timing associated with this local network rhythm may optimize the temporal conditions for excitatory plasticity (21). In contrast, units more likely associated with higher frequency gamma rhythms were suppressed, perhaps corresponding to the reports of high gamma activity as part of an "error" mechanism in vivo (48). Interestingly, the few units that become enhanced in deep cortical layers were those that were significantly more temporally related to these superficial layer enhanced units (Fig. 4*C*). However, the delineation between enhanced and suppressed units, and the high and low gamma frequencies, was not apparent in deep cortical layers. As these layers receive inputs from both layers 2/3 (low gamma) and layer 4 (mainly high gamma) (Fig. 1*B*), further experimentation aimed at quantifying interlaminar cross-frequency coupling is required.

In summary, two distinct forms of synaptic plasticity appeared to influence the pattern of network plasticity, at gamma frequencies, seen on repeated neocortical stimulation. As both were critically dependent on $GABA_B$ receptor activation, it is tempting to suggest that enhancing activity at these receptors may have beneficial effects on cognition. However, the relationship between $GABA_B$ receptor function and cognition is not linear. Enhanced $GABA_B$ signaling is associated with Down syndrome (49) and $GABA_B$ receptor antagonists may enhance (50, 51) or suppress cognitive performance (52). Both excessive and defective $GABA_B$ signaling is associated with similar brain pathology (53). As both excitatory and inhibitory plasticity were dependent on $GABA_B$ receptor function, but in different cortical layers, we suggest that maintaining an appropriate spatial profile of the cognitively critical excitatory–inhibitory synaptic balance in neocortex (54) may be tightly modulated by this aspect of GABAergic signaling.

Methods

Electrophysiology. Horizontal neocortical slices, 450 μm thick, containing primary (Au1) and secondary (Au2) cortex were prepared from adult male Wistar rats (150–250 g). Slices were maintained at 34 °C at the interface between warm wetted 95% (vol/vol) O_2/5% (vol/vol) CO_2 and aCSF containing the following (in millimoles): 3 KCl, 1.25 NaH_2PO_4, 1 $MgSO_4$, 1.2 $CaCl_2$, 24 $NaHCO_3$, 10 glucose, and 126 NaCl. Concurrent recordings of the LFP and extracellular unit activity were made using 10 × 10 Utah electrode arrays (interelectrode distance 0.4 mm) placed covering primary and secondary auditory cortices. Signals were amplified and digitized using either a cyberkinetic amplifier (Blackrock Microsystems) or AlphaLab SnR (AlphaOmega). Both LFP and multiunit data were saved for offline analysis in MATLAB (Mathworks). Additional intracellular and extracellular recordings were taken with sharp microelectrodes filled with 2 M potassium acetate (resistance, 30–90 MΩ) and blunted microelectrodes filled with aCSF (resistance 3–8 MΩ), respectively.

Ascending cortical activation was modeled by focal activation of layer 4 of Au1 using microdrop (approximately 70 nL) application of 1 mM glutamate dissolved in aCSF at the edge of the Utah array (Figs. 1 and 2*A*, *i*). To assess plastic changes in the gamma band and associated spiking activity, two stimuli (same volume, same location) were delivered 1 h apart.

Pyramidal cell inhibitory and excitatory postsynaptic potentials were recorded using sharp intracellular electrodes filled with 2 M KAc, held at −30 mV and −70 mV, respectively, by bipolar electrical stimulation with a width of 0.5 ms at the voltage required to generate half the maximal response. The stimulating electrode was always placed in the same layer as the intracellular recording electrode. Inhibitory responses were recorded in the absence of excitatory ionotropic glutamate responses, ensured by the bath application of glutamate receptor antagonists R-CPP, 3-((*R*)-2-carboxypiperazin-4-yl)-propyl-1-phosphonic acid, (40 μM) and NBQX 2,3-dioxo-6-nitro-1,2,3,4-tetrahydrobenzo[*f*]quinoxaline-7-sulfonamide disodium salt (40 μM). Glutamate receptor antagonists were washed out into aCSF 30 min before activation of cortical layer 4 and reapplied 30 min after stimulation. Poststimulus inhibitory and excitatory responses were then recorded as above 1 h after glutamate application. Neurons recorded for the initial and poststimulus measures of synaptic inhibitory and excitatory responses were not the same, owing to the difficulty in maintaining quality recordings during microdrop application. No significant difference in resting membrane potential or membrane resistance (measures via response to 0.2 nA hyperpolarizing step) was seen for each group ($P > 0.1$, $n = 5$ neurons per layer). All neurons recorded in layers 2/3 and 5 were of the regular spiking subtype. Antagonism of postsynaptic $GABA_B$ receptors was achieved by bath application of CGP 35348 (3-aminopropyl)(diethoxymethyl) phosphinic acid (50 μM), present throughout the entire experiment.

Data Analysis. All electrodes located in cortical and subcortical regions adjacent to Au1 and Au2 were removed before analysis. Remaining data were pooled across all auditory regions. Single units were identified using WaveClus and firing rate was calculated during 1-s bins. The response of single units to each glutamate application was defined as the mean firing rate of a single unit during the initial 10 s of activity following glutamate application. In baseline conditions (before and after each glutamate application) spontaneous spike rates in all layers were low (Fig. 1*C*); however, all response data are represented as spike rate over baseline levels (calculated as the mean over the 10-s period before glutamate application) to compensate for possible lamina-specific differences in background spike rates. Putative pyramidal cells were split into enhanced and suppressed units depending on their mean firing rate during their second response relative to their mean firing rate during the initial response. A "unit plasticity score" was used to quantify overall changes in neuronal activity. The mean number of enhanced or suppressed units recorded per slice was multiplied by the mean, fractional firing rate (second vs. first response to glutamate) for enhanced or suppressed units. Suppressed unit plasticity scores were represented as negative values for clarity in the figures.

LFP data were filtered to remove line noise and bandpass filtered to extract low (30–50 Hz) and high (51–80 Hz) gamma band responses. High and low gamma band activity was then quantified using a fast Fourier transform algorithm on 1-s time bins, and the response to each application of glutamate was defined as the mean integrated power in the relevant frequency band during the initial 10 s of activity postglutamate application for each channel. To examine plastic changes in gamma response, power during both the initial and repeated responses was normalized to 120 s of prestimulus baseline activity (broadband filtered at 20–80 Hz) for each electrode individually before averaging power change above baseline in each layer. These power changes were then compared for the initial and repeated responses. Spike-triggered averages (STAs) of gamma frequency activity were taken ± 150 ms of respective spike timing. Spectra were then calculated from these STAs using a Hamming window. Unit type-specific changes in field potential dynamics were estimated from cross-correlations of these spike-triggered field potential averages. The degree of phase locking of spikes to these STAs was quantified within each gamma subband using CircStat (55).

The relative spike-timing between layers 2/3 and 5/6 was examined by comparing spike trains of populations of enhanced units in layers 2/3 with spikes occurring in populations of enhanced and suppressed units in layers 5/6; the relative spike timing was calculated when spikes in different layers occurred within ±20 ms of each other. Probability distributions were calculated from these relative times using histograms with 2-ms bin widths.

Statistics. Normally distributed data were displayed as mean ± SE mean and statistical differences determined using Student's *t* test. Nonnormally distributed data were displayed as median (IQR), and differences were tested using the Mann–Whitney rank sum test. Laminar differences in the firing rate and distribution of enhanced and suppressed units were tested with one-way ANOVA, using Bonferroni's method for even groups (unit distribution) and Dunn's method for uneven groups (firing rate). Frequency-dependent statistical comparisons of the spike-triggered averages between enhanced and suppressed single units were calculated as follows: A bootstrap procedure was used to generate surrogate data for the null hypothesis (no difference between coherence of enhanced and suppressed units). The empirical difference in coherence was then compared with the surrogate data for each frequency bin and corrected for multiple comparisons using false discovery rate. Significance was set at the 5% level.

ACKNOWLEDGMENTS. We thank M. Kramer and U. Eden for assistance with the Monte Carlo time-series comparisons. This work was funded by the Wellcome Trust and the Engineering and Physical Sciences Research Council CARMEN e-science project, along with National Science Foundation (NSF) DMS 1042134 and NSF DMS 1225647. S.L. was supported by an NIH Institutional Training Grant (5T32MH019118-23).

1. Gray CM, König P, Engel AK, Singer W (1989) Oscillatory responses in cat visual cortex exhibit inter-columnar synchronization which reflects global stimulus properties. *Nature* 338(6213):334–337.
2. Fries P (2005) A mechanism for cognitive dynamics: Neuronal communication through neuronal coherence. *Trends Cogn Sci* 9(10):474–480.
3. Gruber T, Giabbiconi CM, Trujillo-Barreto NJ, Muller MM (2006) Repetition suppression of induced gamma band responses is eliminated by task switching. *Eur J Neurosci* 24(9):2654–2660.
4. Todorovic A, van Ede F, Maris E, de Lange FP (2011) Prior expectation mediates neural adaptation to repeated sounds in the auditory cortex: An MEG study. *J Neurosci* 31(25):9118–9123.
5. Brunet NM, et al. (2014) Stimulus repetition modulates gamma-band synchronization in primate visual cortex. *Proc Natl Acad Sci USA* 111(9):3626–3631.
6. Miller EK, Li L, Desimone R (1991) A neural mechanism for working and recognition memory in inferior temporal cortex. *Science* 254(5036):1377–1379.
7. Kaliukhovich DA, Vogels R (2011) Stimulus repetition probability does not affect repetition suppression in macaque inferior temporal cortex. *Cereb Cortex* 21(7): 1547–1558.
8. Ainsworth M, et al. (2012) Rates and rhythms: A synergistic view of frequency and temporal coding in neuronal networks. *Neuron* 75(4):572–583.
9. Uhlhaas PJ, Pipa G, Neuenschwander S, Wibral M, Singer W (2011) A new look at gamma? High- (>60 Hz) γ-band activity in cortical networks: Function, mechanisms and impairment. *Prog Biophys Mol Biol* 105(1-2):14–28.
10. Conrad N, Giabbiconi CM, Müller MM, Gruber T (2007) Neuronal correlates of repetition priming of frequently presented objects: Insights from induced gamma band responses. *Neurosci Lett* 429(2-3):126–130.
11. Masamizu Y, et al. (2014) Two distinct layer-specific dynamics of cortical ensembles during learning of a motor task. *Nat Neurosci* 17(7):987–994.
12. Miller EK, Desimone R (1994) Parallel neuronal mechanisms for short-term memory. *Science* 263(5146):520–522.
13. Gruber T, Müller MM (2005) Oscillatory brain activity dissociates between associative stimulus content in a repetition priming task in the human EEG. *Cereb Cortex* 15(1): 109–116.
14. Cohen NJ, Squire LR (1980) Preserved learning and retention of pattern-analyzing skill in amnesia: Dissociation of knowing how and knowing that. *Science* 210(4466): 207–210.
15. Desimone R (1996) Neural mechanisms for visual memory and their role in attention. *Proc Natl Acad Sci USA* 93(24):13494–13499.
16. Wiggs CL, Martin A (1998) Properties and mechanisms of perceptual priming. *Curr Opin Neurobiol* 8(2):227–233.
17. Gotts SJ, Chow CC, Martin A (2012) Repetition priming and repetition suppression: A case for enhanced efficiency through neural synchronization. *Cogn Neurosci* 3(3–4): 227–237.
18. Pluta S, et al. (2015) A direct translaminar inhibitory circuit tunes cortical output. *Nat Neurosci* 18(11):1631–1640.
19. Collingridge GL, Singer W (1990) Excitatory amino acid receptors and synaptic plasticity. *Trends Pharmacol Sci* 11(7):290–296.
20. Whittington MA, Cunningham MO, LeBeau FEN, Racca C, Traub RD (2011) Multiple origins of the cortical γ rhythm. *Dev Neurobiol* 71(1):92–106.
21. Lee S, Sen K, Kopell N (2009) Cortical gamma rhythms modulate NMDAR-mediated spike timing dependent plasticity in a biophysical model. *PLOS Comput Biol* 5(12): e1000602.
22. Bear MF, Malenka RC (1994) Synaptic plasticity: LTP and LTD. *Curr Opin Neurobiol* 4(3):389–399.
23. Kullmann DM, Moreau AW, Bakiri Y, Nicholson E (2012) Plasticity of inhibition. *Neuron* 75(6):951–962.
24. Ainsworth M, et al. (2011) Dual γ rhythm generators control interlaminar synchrony in auditory cortex. *J Neurosci* 31(47):17040–17051.
25. Mott DD, Lewis DV (1991) Facilitation of the induction of long-term potentiation by $GABA_B$ receptors. *Science* 252(5013):1718–1720.
26. Komatsu Y (1996) $GABA_B$ receptors, monoamine receptors, and postsynaptic inositol trisphosphate-induced Ca2+ release are involved in the induction of long-term potentiation at visual cortical inhibitory synapses. *J Neurosci* 16(20):6342–6352.
27. Gilbert JR, Gotts SJ, Carver FW, Martin A (2010) Object repetition leads to local increases in the temporal coordination of neural responses. *Front Hum Neurosci* 4:30.
28. Grill-Spector K, Henson R, Martin A (2006) Repetition and the brain: Neural models of stimulus-specific effects. *Trends Cogn Sci* 10(1):14–23.
29. von Stein A, Chiang C, König P (2000) Top-down processing mediated by interareal synchronization. *Proc Natl Acad Sci USA* 97(26):14748–14753.
30. Ghuman AS, Bar M, Dobbins IG, Schnyer DM (2008) The effects of priming on frontal-temporal communication. *Proc Natl Acad Sci USA* 105(24):8405–8409.
31. Traub RD, Bibbig A, LeBeau FE, Cunningham MO, Whittington MA (2005) Persistent gamma oscillations in superficial layers of rat auditory neocortex: Experiment and model. *J Physiol* 562(Pt 1):3–8.
32. Atallah BV, Scanziani M (2009) Instantaneous modulation of gamma oscillation frequency by balancing excitation with inhibition. *Neuron* 62(4):566–577.
33. Whittington MA, Traub RD, Faulkner HJ, Stanford IM, Jefferys JG (1997) Recurrent excitatory postsynaptic potentials induced by synchronized fast cortical oscillations. *Proc Natl Acad Sci USA* 94(22):12198–12203.
34. Kuenzi FM, Fitzjohn SM, Morton RA, Collingridge GL, Seabrook GR (2000) Reduced long-term potentiation in hippocampal slices prepared using sucrose-based artificial cerebrospinal fluid. *J Neurosci Methods* 100(1–2):117–122.
35. Davies CH, Starkey SJ, Pozza MF, Collingridge GL (1991) GABA autoreceptors regulate the induction of LTP. *Nature* 349(6310):609–611.
36. Pi HJ, et al. (2013) Cortical interneurons that specialize in disinhibitory control. *Nature* 503(7477):521–524.
37. Oláh S, et al. (2009) Regulation of cortical microcircuits by unitary GABA-mediated volume transmission. *Nature* 461(7268):1278–1281.
38. Kampa BM, Letzkus JJ, Stuart GJ (2006) Cortical feed-forward networks for binding different streams of sensory information. *Nat Neurosci* 9(12):1472–1473.
39. Sjöström PJ, Häusser M (2006) A cooperative switch determines the sign of synaptic plasticity in distal dendrites of neocortical pyramidal neurons. *Neuron* 51(2):227–238.
40. Meredith RM, Floyer-Lea AM, Paulsen O (2003) Maturation of long-term potentiation induction rules in rodent hippocampus: Role of GABAergic inhibition. *J Neurosci* 23(35):11142–11146.
41. Nusser Z, Hájos N, Somogyi P, Mody I (1998) Increased number of synaptic GABA(A) receptors underlies potentiation at hippocampal inhibitory synapses. *Nature* 395(6698):172–177.
42. Maffei A, Nataraj K, Nelson SB, Turrigiano GG (2006) Potentiation of cortical inhibition by visual deprivation. *Nature* 443(7107):81–84.
43. Sudhakaran IP, et al. (2012) Plasticity of recurrent inhibition in the Drosophila antennal lobe. *J Neurosci* 32(21):7225–7231.
44. Wang L, Maffei A (2014) Inhibitory plasticity dictates the sign of plasticity at excitatory synapses. *J Neurosci* 34(4):1083–1093.
45. Lourenço J, et al. (2014) Non-associative potentiation of perisomatic inhibition alters the temporal coding of neocortical layer 5 pyramidal neurons. *PLoS Biol* 12(7): e1001903.
46. D'amour JA, Froemke RC (2015) Inhibitory and excitatory spike-timing-dependent plasticity in the auditory cortex. *Neuron* 86(2):514–528.
47. Martens U, Gruber T (2012) Sharpening and formation: Two distinct neuronal mechanisms of repetition priming. *Eur J Neurosci* 36(7):2989–2995.
48. Rothé M, Quilodran R, Sallet J, Procyk E (2011) Coordination of high gamma activity in anterior cingulate and lateral prefrontal cortical areas during adaptation. *J Neurosci* 31(31):11110–11117.
49. Best TK, Siarey RJ, Galdzicki Z (2007) Ts65Dn, a mouse model of Down syndrome, exhibits increased GABAB-induced potassium current. *J Neurophysiol* 97(1):892–900.
50. Pitsikas N, Rigamonti AE, Cella SG, Muller EE (2003) The $GABA_B$ receptor and recognition memory: Possible modulation of its behavioral effects by the nitrergic system. *Neuroscience* 118(4):1121–1127.
51. Helm KA, et al. (2005) $GABA_B$ receptor antagonist SGS742 improves spatial memory and reduces protein binding to the cAMP response element (CRE) in the hippocampus. *Neuropharmacology* 48(7):956–964.
52. Cryan JF, et al. (2004) Behavioral characterization of the novel GABAB receptor-positive modulator GS39783 (N,N′-dicyclopentyl-2-methylsulfanyl-5-nitro-pyrimidine-4,6-diamine): Anxiolytic-like activity without side effects associated with baclofen or benzodiazepines. *J Pharmacol Exp Ther* 310(3):952–963.
53. Bowery NG (2006) $GABA_B$ receptor: A site of therapeutic benefit. *Curr Opin Pharmacol* 6(1):37–43.
54. Froemke RC (2015) Plasticity of cortical excitatory-inhibitory balance. *Annu Rev Neurosci* 38:195–219.
55. Berens P (2009) Circstat: A matlab toolbox for circular statistics. *J Stat Softw* 31:10.